Experimental and Molecular Pathology 110 (2019) 104275

Contents lists available at ScienceDirect

Experimental and Molecular Pathology

journal homepage: www.elsevier.com/locate/yexmp

Acute corneal injury in rabbits following nitrogen mustard ocular exposure

Dinesh G. Goswami[a], Rama Kant[a], David A. Ammar[b,1], Dileep Kumar[a], Robert W. Enzenauer[b], J. Mark Petrash[a,b], Neera Tewari-Singh[a,2], Rajesh Agarwal[a,*]

[a] Department of Pharmaceutical Sciences, University of Colorado, Anschutz Medical Campus, Aurora, CO 80045, USA
[b] Department of Ophthalmology, University of Colorado, Anschutz Medical Campus, Aurora, CO 80045, USA

ARTICLE INFO

Keywords:
Sulfur mustard
Nitrogen mustard
Vesicant
Mustard
Corneal injury
Inflammation

ABSTRACT

Sulfur mustard (SM), a potent vesicating chemical warfare agent, and its analog nitrogen mustard (NM), are both strong bi-functional alkylating agents. Eyes, skin, and the respiratory system are the main targets of SM and NM exposure; however, ocular tissue is most sensitive, resulting in severe ocular injury. The mechanism of ocular injury from vesicating agents' exposure is not completely understood. To understand the injury mechanism from exposure to vesicating agents, NM has been previously employed in our toxicity studies on primary human corneal epithelial cells and *ex vivo* rabbit cornea organ culture model. In the current study, corneal toxicity from NM ocular exposure (1%) was analyzed for up to 28 days post-exposure in New Zealand White male rabbits to develop an acute corneal injury model. NM exposure led to conjunctival and eyelid swelling within a few hours after exposure, in addition to significant corneal opacity and ulceration. An increase in total corneal thickness and epithelial degradation was observed starting at day 3 post-NM exposure, which was maximal at day 14 post-exposure and did not resolve until 28 days post-exposure. There was an NM-induced increase in the number of blood vessels and inflammatory cells, and a decrease in keratocytes in the corneal stroma. NM exposure resulted in increased expression levels of cyclooxygenase-2, Interleukin-8, vascular endothelial growth factor and Matrix Metalloproteinase 9 indicating their involvement in NM-induced corneal injury. These clinical, biological, and molecular markers could be useful for the evaluation of acute corneal injury and to screen for therapies against NM- and SM-induced ocular injury.

1. Introduction

Vesicating chemical warfare agents cause severe respiratory, skin, and ocular injuries (Ghabili et al., 2011; Ghabili et al., 2010; Papirmeister et al., 1991). Due to their easy synthesis and low cost of manufacturing in comparison with conventional weapons, vesicating agents are of potential threat as warfare agents and as terrorist weapons (Geraci, 2008; Wattana and Bey, 2009). The most common vesicating agents include sulfur mustard (SM), nitrogen mustard (NM), arsenical vesicant lewisite (LEW), and nettle agent phosgene oxime (CX) (WHO, 2004). Among vesicating agents, SM has been most widely used in warfare resulting in injuries and battlefield causalities (Balali-Mood et al., 2011; Balali-Mood and Hefazi, 2006; Geraci, 2008; Mansour Razavi et al., 2012; Saladi et al., 2006; Smith and Skelton, 2003). The eye is the most sensitive tissue to SM exposure, with symptoms (photophobia, foreign body sensation, lacrimation, blepharospasm, and corneal ulceration) appearing 2-6 h after exposure and healing within few weeks. However, in some cases delayed injury symptoms (dryness, conjunctival scarring, decreased visual acuity, persistent corneal defects, inflammation, and neovascularization) develop, leading to progressive visual deterioration (Balali-Mood and Hefazi, 2006; Ghasemi et al., 2009; Ghasemi et al., 2013; Gordon et al., 2009; Kadar et al., 2009; McNutt et al., 2012).

In spite of several studies on toxic effects of SM, the mechanism of ocular injury from SM is not fully understood. There are no approved therapies and the treatment is mostly symptomatic management

Abbreviations: SM, sulfur mustard; NM, nitrogen mustard; HCE, human corneal epithelial cells; COX2, cyclooxygenase 2; MMPs, matrix metalloproteinase; VEGF, vascular endothelial growth factor; LSCD, limbal stem cell deficiency; MAPK, mitogen activated protein kinases; LEW, lewisite; CX, phosgene oxime; ROS, reactive oxygen species

* Corresponding author at: Skaggs School of Pharmacy and Pharmaceutical Sciences, University of Colorado, Anschutz Medical Campus, Mail Stop C238, 12850 E. Montview Blvd., Room V20-2118, Aurora, CO 80045, USA.
E-mail address: Rajesh.Agarwal@ucdenver.edu (R. Agarwal).
[1] Current address: Lions Eye Institute for Transplant and Research, Tampa, FL 33605, USA.
[2] Current address: Department of Pharmacology and Toxicology, Michigan State University, East Lansing, MI 48824, USA.

https://doi.org/10.1016/j.yexmp.2019.104275
Received 23 April 2019; Received in revised form 22 May 2019
Available online 21 June 2019

Table 1
Scoring system for clinical study parameters.

Clinical parameter	Score (grade)	Definition
Corneal stromal injury (opacity)	0	Cornea transparent
	1	Minimal loss of corneal transparency
	2	Moderate loss of corneal transparency – iris vessels and pupil still visible
	3	Severe loss of corneal transparency – either iris vessels or pupil not visible
	4	Diffuse loss of corneal transparency – neither iris vessels nor pupil visible
Corneal ulceration	0	Corneal ulceration not present
	1	Corneal ulceration (< 25% of the cornea)
	2	Corneal ulceration (25–50% of the cornea)
	3	Corneal ulceration (50–75% of the cornea)
	4	Corneal ulceration (> 75% of the cornea)

(Ghasemi et al., 2013; Gordon et al., 2016; Goswami et al., 2016a; Horwitz et al., 2014; Kadar et al., 2014; McNutt et al., 2012; Panahi et al., 2017). SM is lipophilic in nature, and after penetrating the epithelium can lead to local and systemic adverse effects (Kehe and Szinicz, 2005). SM is highly reactive. While formation of DNA adducts is considered one of the major lesions, other mechanisms leading to SM toxicity include oxidative stress, increased matrix metalloproteinases (MMPs) activity, upregulation of pro-inflammatory cytokines and loss of endothelial cells and limbal stem cell deficiency (Gordon et al., 2009; Goswami et al., 2016b; Kadar et al., 2009; Kadar et al., 2013; Kadar et al., 2011; Kehe et al., 2009). However, efforts are still required to understand the complete underlying injury mechanism and to develop safe and effective therapies.

NM is a bi-functional analogue of SM and has been used to study vesicating agents-induced ocular injuries (Anumolu et al., 2010; Banin et al., 2003; Gordon et al., 2010; Goswami et al., 2016b; Morad et al., 2005; Tewari-Singh et al., 2012). In this regard, previously we have reported the effects of NM exposure on HCE cells and *ex vivo* rabbit cornea organ culture (Goswami et al., 2016b; Tewari-Singh et al., 2012). Compared to SM, NM exposure results in similar injury (although less severe), is commercially available, and poses a similar potential threat of exposure. In the HCE cells, NM exposure resulted in cell death, increase in DNA damage, apoptotic cell death markers, inflammatory mediators, activation of MAPKs, and lipid peroxidation and protein oxidation (Goswami et al., 2016b). In the *ex vivo* cornea culture, NM exposure caused cell death, epithelial-stromal separation and increase in the levels of cyclooxygenase 2 (COX-2), proteolytic mediator MMP-9, and vascular endothelial growth factor (VEGF) in cultured rabbit corneas (Goswami et al., 2018; Tewari-Singh et al., 2012). Following up on our previous cell culture and *ex vivo* study reports, in the present study, we examined the *in vivo* ocular toxic effects of NM (1% NM exposure for 5 min) in rabbit (New Zealand White) model. The clinical and pathophysiological effects of NM exposure were evaluated during a 28-day post exposure period to establish useful clinical, biological, and molecular markers for the progression of injury. These would be helpful in understanding the injury mechanism and the elucidation of underlying pathways. Together, these could be useful for future designing, screening, and evaluation of possible therapeutic agents for treating NM and SM-induced ocular injuries.

2. Materials and methods

2.1. Exposure of rabbit eyes to NM

All the animal experiments were conducted in accordance with the National Institutes of Health guidelines for the care and use of laboratory animals. Following a protocol approved by the institutional IACUC, male New Zealand white rabbits (4-5 lbs) were procured from Charles River Laboratories. After a quarantine and acclimation period, animals were randomly divided into different groups ($n = 3$ each group) for NM exposure. Buprenorphine-SR LAB (0.15 mg/Kg sq) was given a day before NM exposures for pain management and was given every 72 h thereafter as needed. On the day of the NM exposure, rabbits were anesthetized with a subcutaneous administration of ketamine (12.5 mg/kg) and xylazine (2.5 mg/kg). Retrobulbar block using bupivacaine was also carried out to ease pain from the procedure. Once anesthetized, a 14 mm non-sharp trephine was put between the eyelids under a biosafety cabinet. The right eye was exposed to NM (100 µL of 1% NM for 5 min) while the left eye was exposed to saline (100 µL of saline for 5 min) and served as control After the exposure the eyes were gently rinsed with saline and the rabbit was placed in a clean container until being sternal before transport to housing room and provided food and water *ad libitum*.

2.2. Evaluation of corneal-stromal injury (corneal opacity) and corneal ulceration

The rabbits were monitored closely and assessment of pain/discomfort signs including: hunched posture, altered activity level, tearing, grinding of teeth, covering of eyes with front feet and menace response was carried out. Whole eye injury was observed, and digital pictures were taken at day 3,7, 14, 21, and 28 post NM-exposure. Similarly, clinical evaluations for corneal stromal injury (corneal opacity) and corneal ulceration were carried out at day 3, 7, 14, 21, and 28 post NM-exposure using slit lamp imaging (following the scoring system listed in Table 1). The rabbits were sacrificed at day 3, 14, and 28 post NM-exposure and the cornea was dissected and was either snap frozen in liquid nitrogen or fixed in formalin for further studies.

2.3. Histopathological evaluation and measurement of corneal and epithelial thickness, epithelial-degradation, and epithelial-stromal separation

The formalin fixed corneas were processed, and paraffin embedded. Five micrometer thick sections were cut and stained with hematoxylin and eosin (H&E) as reported earlier (Tewari-Singh et al., 2012). The H&E stained sections were evaluated microscopically for corneal thickness, epithelial thickness, epithelial-degradation, and epithelial-stromal separation as reported earlier (Tewari-Singh et al., 2017). Briefly, corneal thickness from 10 to 12 randomly selected corneal areas was measured (~1.0 mm away from both the sides of the cornea and the limbus region at 100× magnification) in each cornea. The epithelial thickness was measured in at least five randomly selected fields throughout the length of the cornea and five measurements were carried out from each field at 400× magnification. Epithelial degradation and epithelial-stromal separation was measured in whole length (~7 mm) of the cornea at 400× magnification.

2.4. Evaluation of stroma for the measurement of keratocytes, inflammatory cells, and blood vessels

The H&E stained rabbit cornea sections were evaluated microscopically and quantification of number of keratocytes, inflammatory

cells, and blood vessels in the stroma was carried out. Keratocyte quantification was carried out in ~ 7 mm^2 of the stroma and average in 1 mm^2 was calculated. The number of blood vessels and inflammatory cells were quantified from whole stromal region of the cornea. The density of inflammatory cells was scored as 1, < 50; 2, 50–100; 3, 100–500; 4, > 500 inflammatory cells.

2.5. Immunohistochemistry (IHC) for vascular endothelial growth factor (VEGF), Cyclooxygenase-2 (COX-2) and Matrix metalloproteinase-9 (MMP-9)

IHC for COX-2, MMP-9, and VEGF was carried out on corneal sections as described previously (Tewari-Singh et al., 2012). Briefly, corneal sections from control and NM-exposed eyes were subjected to antigen retrieval and blocking of endogenous peroxidase activity. Thereafter, the sections were incubated with anti-VEGF (Abcam, Cambridge, MA; ab28775; 1:250 dilution), anti-COX-2 (Cayman Chemicals, Ann Arbor, MI; 160112; 1:500 dilution), or anti MMP-9 (Abcam, Cambridge, MA; ab58803; 1:500) antibodies, followed by incubation with biotinylated secondary antibody (DAKO, Santa Clara, CA; E043301; 1:500 dilution) and streptavidin-HRP conjugated antibody (GE Healthcare, Waukesha, WI; RPN1231; 1:500 dilution). Rabbit IgG antibody (N-Universal, DAKO, Santa Clara, CA) was used as negative control. The sections were then incubated in DAB and counterstained with diluted hematoxylin. The brown colored cytoplasmic staining was scored as positivity score in 10 randomly selected fields (at 400× magnification). The intensity of brown colour was scored as 0 (no staining), +1 (weak staining), +2 (moderate staining), +3 (strong staining), and + 4 (very strong staining).

2.6. Analyses of IL-8 and MMP-9 in corneal lysates

IL-8 and MMP-9 levels were analyzed in corneal tissue lysate samples (n = 3, 3-day post NM-exposed samples) from NM exposed eyes. The lysates were subjected to G-series Rabbit Cytokine Array from Ray Biotech (Norcross, GA) according to the suggested protocol. Briefly, the array surface was blocked with the sample diluent followed by incubation with the samples. After washing, biotinylated detection antibody was added followed by washing and incubation with Cy3 equivalent dye-conjugated streptavidin. Raybiotech scanning services were used for slide scanning and data extraction and the data was analyzed using Raybiotech array specific data analysis software. The data was plotted as relative fluorescence unit (mean ± SEM).

2.7. Statistical analysis

Data was analyzed using one-way analysis of variance (one-way ANOVA) to get the statistically significant difference in control *versus* NM exposed groups, with Tukey or Bonferroni t-test for multiple comparisons (Sigma Stat 2.03). Differences were considered significant if the p value was < 0.05. Data are presented as the mean ± standard error of mean (SEM).

3. Results

3.1. NM exposure caused corneal opacity and corneal ulceration

Corneal injury parameters including corneal-stromal injury (corneal opacity) and corneal ulceration were evaluated *via* slit lamp examinations by the authors upon NM exposure in rabbit eyes. Corneal opacity was evaluated as the loss of transparency (Table 1). NM exposure induced severe eyelid and conjunctival swelling due to which rabbits had difficulty in opening their eyes, and the corneal opacity could not be measured at day 1 post-NM exposure. The swelling was still very pronounced at day 3 post-NM exposure (Fig. 1A). At day-3 post NM-exposure, the loss of corneal transparency was severe with either iris or

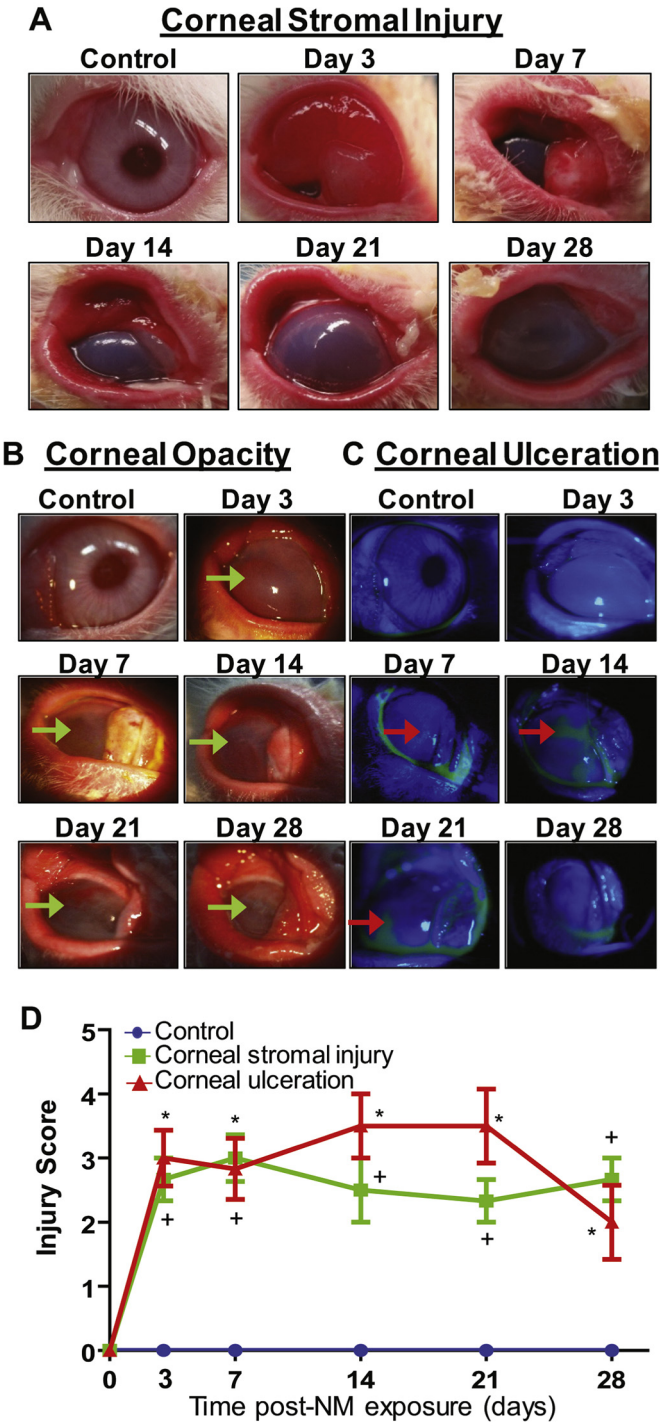

Fig. 1. Clinical progression of ocular injury following NM exposure. Right eye of New Zealand white rabbits was exposed to NM (1%) for 5 min and the left eye was exposed to saline and clinical progression of injury was observed for 28 days post-exposure as detailed in the "Materials and methods" section. Representative pictures showing injury to the rabbit eyes and the progression of ocular injury following NM exposure (A). Representative Slit lamp pictures showing corneal opacity (B), and corneal ulceration (C) following NM exposure. Green arrows, scarring or clouding of cornea or corneal opacity; red arrows, corneal ulceration; fluorescein stain taken up by exposed stroma, due to the disruption of epithelial layer, appears green. Quantification of corneal-stromal injury and corneal ulceration (D). Control (blue line) represents both corneal-stromal injury and corneal ulceration. Data presented are mean ± SEM (n = 3–6). +, $p < 0.05$ compared to the control group (corneal stromal injury); *, $p < 0.05$ compared to the control group (corneal ulceration). (For interpretation of the references to colour in this figure legend, the reader is referred to the web version of this article.)

pupil not visible. The corneal opacity was maximal at day 7 post-exposure and decreased marginally thereafter till day 21 post-exposure before a slight increase observed again at day 28 post-exposure (green arrows, Fig. 1B). Fluorescein (green) staining due to depleted epithelial layer was also measured as an indicator of corneal ulceration (red arrows, Fig. 1C). A significant increase in corneal ulceration ($p < 0.05$; with 50–75% cornea staining positive for fluorescein) was observed at day 3 post NM-exposure, which was maximal between day 14 and 21 post-exposure (> 75% of cornea staining positive for fluorescein) before a small decrease (25–50% of the cornea staining with fluorescein) was observed at day 28 post NM-exposure (Fig. 1C & D).

3.2. NM exposure caused an increase in corneal thickness and induced epithelial degradation and epithelial-stromal separation

Corneal thickness was evaluated in the H&E stained corneal sections. NM exposure caused an increase in corneal thickness, with thickness more than doubling as compared to the control at day 3 post NM-exposure (corneal thickness was 715 µm in NM-exposed group compared to 346 µm in control group). The corneal thickness was maximal at day 14 post NM-exposure (corneal thickness was 2.6-fold higher in NM exposed group compared to the control group animals) and was still pronounced (2.3-fold higher) in NM exposed group compared to control at day 28 post-exposure (Fig. 2A).

Corneal sections were analyzed for the effect of NM exposure on the epithelial layer. NM ocular exposure lead to significant ($p < 0.05$) corneal epithelial degradation (the epithelial thickness was reduced by approximately 50% (17.8 µm in NM exposed group compared to 36 µm in control group animals) at day 3 post-exposure. The decrease in epithelial thickness (epithelial degradation) was maximal at day 14 post-exposure (epithelial thickness reduced to ~20% as compared to that of control; 7.2 µm in NM exposed group compared to 32 µm in control group). Compared to day 14, epithelial thickness in NM-exposed eyes recovered somewhat by day 28 (Fig. 2B), although epithelial thinning was still very pronounced compared to controls.

Epithelial-stromal separation is a hallmark of vesicant exposure in skin tissue. In our studies, NM exposure did induce epithelial-stromal separation (2–3% of the total length of the cornea), however, the separations were not significant compared to the control (Fig. 2C). The large variability was observed among samples from this group, possibly related to variable recovery of tissues damaged by exposure to NM.

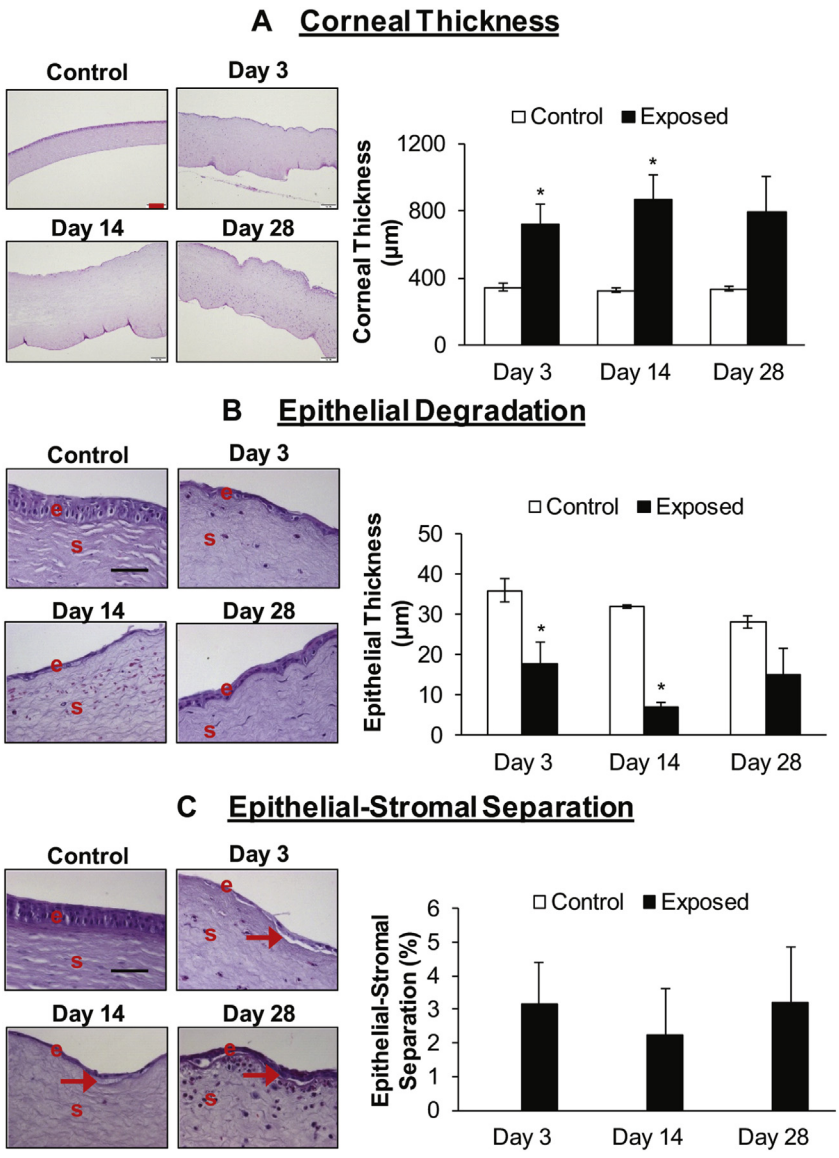

Fig. 2. Effect of NM exposure on corneal thickness (A), epithelial degradation (B), and epithelial-stromal separation (C). Right eye of New Zealand white rabbits was exposed to NM (1%) for 5 min and the left eye was exposed to saline. The rabbits were euthanized at days 3, 14, and 28 post NM-exposure, the eyes were dissected, and the corneal tissue was fixed for histopathologic evaluation. The total corneal thickness, epithelial degradation, and epithelial-stromal separation in the hematoxylin and eosin (H&E) stained corneal sections was measured as detailed under the "Materials and Methods" section. Representative images showing corneal thickness and bar diagram showing quantitative data from the measurement of the corneal thickness (A) in control and NM exposed corneal sections. Representative images showing epithelial-degradation and bar diagram showing quantification of the epithelial-degradation (B) in control and NM exposed corneal sections. Representative images showing epithelial-stromal separation and bar diagram showing quantification of the epithelial- stromal separation (C; no control bars indicate that there was no epithelial-stromal separation in control corneas). Representative control images are from 3-day post NM exposure. Data presented are mean ± SEM (n = 3). *, $p < 0.05$ compared to the control group. e, epithelium; s, stroma; red arrows, epithelial-stromal separation; red size bar (corneal thickness), 200 µm; black size bar (epithelial degradation and epithelial-stromal separation), 50 µm. (For interpretation of the references to colour in this figure legend, the reader is referred to the web version of this article.)

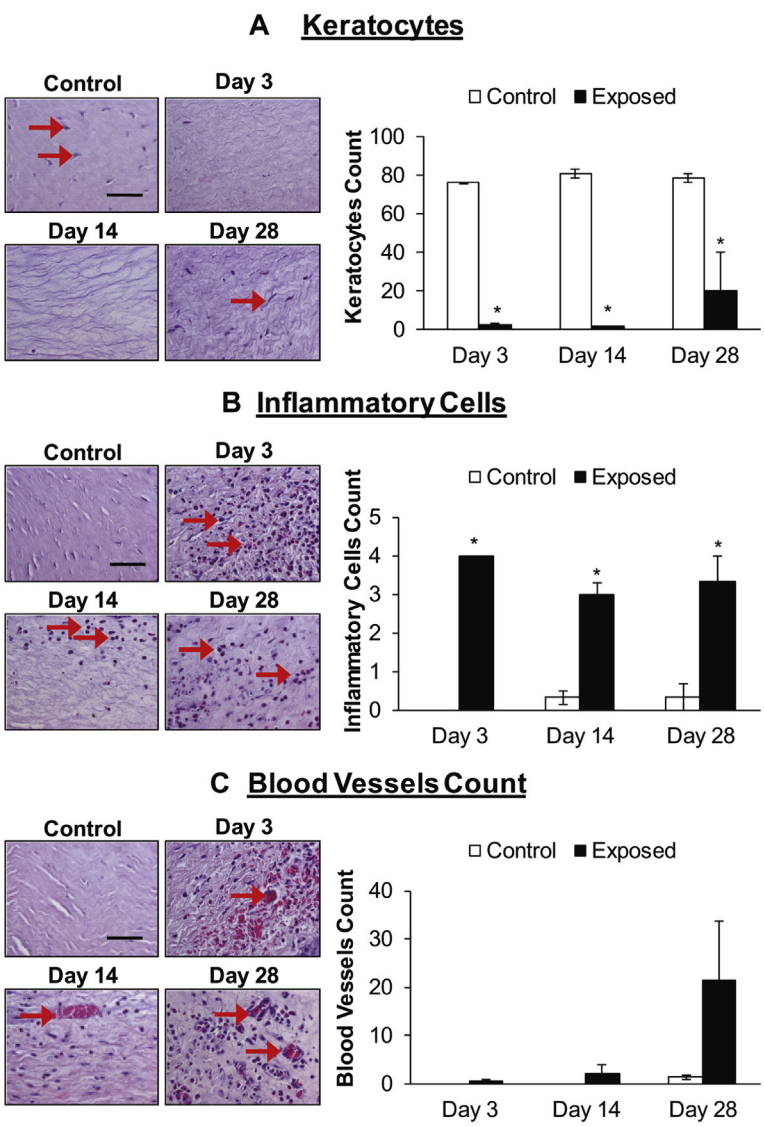

Fig. 3. NM exposure causes a decrease in the number of keratocyte (A), and an increase in the number of inflammatory cells (B) and blood vessels (C) in the stroma of rabbit cornea. Right eye of New Zealand white rabbits was exposed to NM (1%) for 5 min and the left eye was exposed to saline. The rabbits were euthanized at days 3, 14, and 28 post NM-exposure, the eyes were dissected, and the corneal tissue was fixed for histopathologic evaluation. The corneal sections were H&E stained and number of keratocytes, inflammatory cells, and blood vessels were quantified as detailed under the "Materials and Methods" section. Representative images showing a decrease in keratocytes and bar diagram showing the quantification of keratocytes in the stroma (A). Representative images showing an increase in the inflammatory cells in the corneal stroma following NM exposure and bar diagram showing the quantification of inflammatory cells (B; no control bars at day 3 indicate that there was no significant inflammatory cell infiltration observed in the control corneas) detailed under the material and methods section. Representative images showing an increase in number of blood vessels in the corneal stroma and bar diagram showing the quantification of blood vessels (C; no control bars at day 3 and day 14 indicate that blood vessels in the control corneas were not observed at these time points). Representative control images are from 3-day post NM exposure. Data presented are mean ± SEM (n = 3); *, $p < 0.05$ compared to the control group. e, epithelium; s, stroma; red arrows, keratocytes/inflammatory cells/blood vessels; size bar, 50 μm. (For interpretation of the references to colour in this figure legend, the reader is referred to the web version of this article.)

3.3. NM exposure decreased number of keratocytes and caused influx of inflammatory cells, and increase in blood vessels in the stroma of the rabbit cornea

NM exposure caused a decrease in the number of keratocytes throughout the stromal region of the rabbit corneas. At day 3 and 14 post-exposure, the stroma was almost devoid of keratocytes (Fig. 3A, red arrows). At day 28 post NM-exposure the keratocytes began to re-appear, although their number was still only ~25% of that observed in control corneas (Fig. 3A). The H&E stained corneal sections were evaluated for the influx of inflammatory cells/inflammatory response. NM exposure resulted in a significant ($p < 0.05$) influx of inflammatory cells in the stroma at all the study time points (Fig. 3B; red arrows) with maximal increase at day 3 post NM-exposure. At day 14, a decrease in the number of inflammatory cells was observed compared to day 3 before increasing again at day 28 post NM-exposure (Fig. 3B). NM-exposure also led to an increase in the number of blood vessels in the stroma of the cornea with maximal increase at day 28 post-exposure (Fig. 3C, red arrows), however this increase was not statistically significant compared to the control.

3.4. NM-exposure led to increased expression of COX-2, IL-8, MMP-9, and VEGF in the rabbit cornea

Since an influx of inflammatory cells was observed in the H&E stained corneal tissue, we next analyzed the expression of inflammatory marker COX-2 and changes in other inflammatory cytokines upon NM exposure. An increase in the COX-2 expression was observed at day 3 with maximal staining observed at day 14 post NM-exposure. However, there was substantial epithelial degradation (epithelial layer was reduced to single cell layer), because of which the staining was not prominent and difficult to grade (Fig. 4A). Cytokine analyses using rabbit cytokine array revealed a significant increase in IL-8 expression upon NM-exposure (~21-fold increase in IL-8 levels in NM exposed group compared to the control group) in rabbit cornea at day 3 post NM-exposure (Fig. 4B). MMP-9, which is known play an important role in vesicating agents-induced blister formation and epithelial-stromal separation, was also analyzed. An increase in the intensity of MMP-9 staining was observed (Fig. 4C), again due to decrease in thickness of the epithelial layer the IHC staining was difficult to evaluate and grade. Analyses of MMP-9 using cytokine array showed a significant increase in MMP-9 levels (11.7-fold increase in MMP-9 levels in NM exposed group compared to the control group) at 3-day post NM-exposure (Fig. 4D). Levels of the angiogenic factor VEGF, which was found to be increased upon NM-exposure in HCE cells and *ex vivo* rabbit cornea,

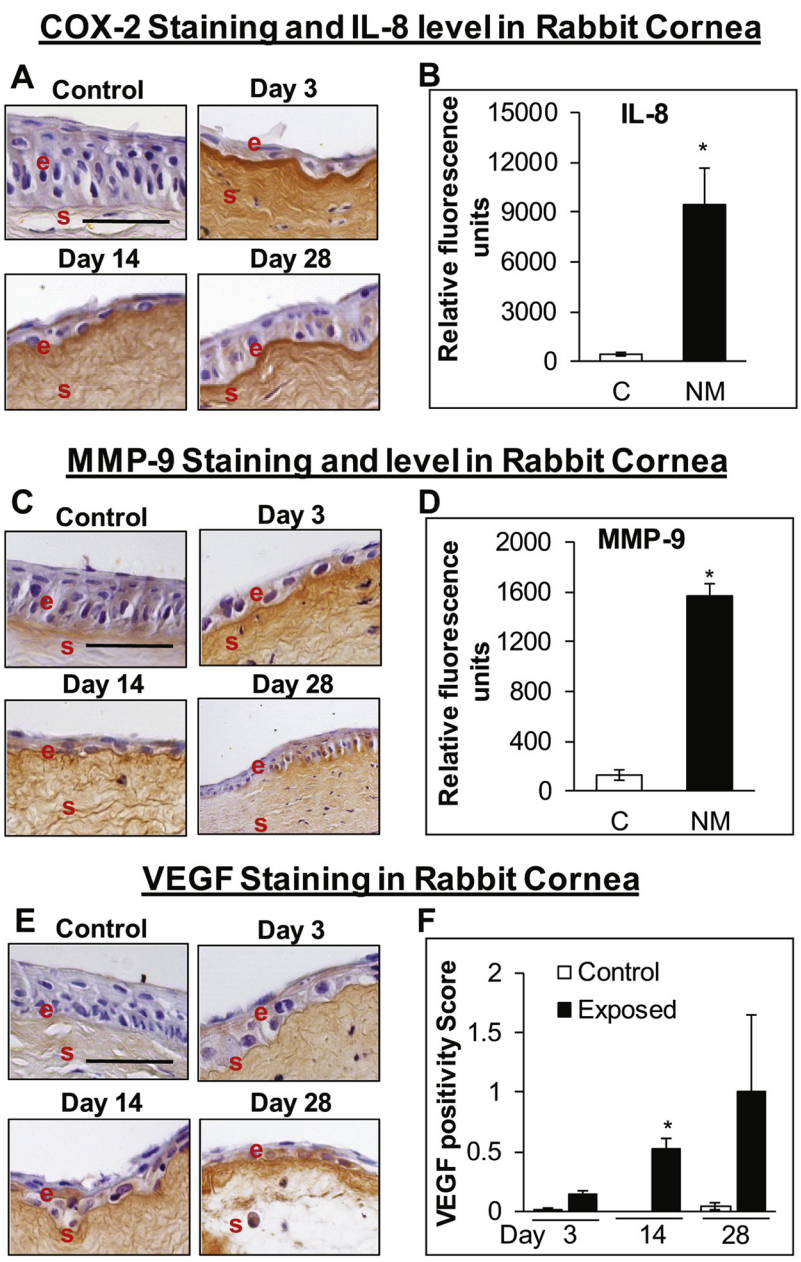

Fig. 4. NM exposure causes an increase in the expression of COX-2 (A), MMP-9 (B), and VEGF (C) expression in rabbit cornea. Right eye of New Zealand white rabbits was exposed to NM (1%) for 5 min and the left eye was exposed to saline. The rabbits were euthanized at days 3, 14, and 28 post-NM exposure, the eyes were dissected, and were either fixed for immunohistochemistry (IHC) evaluation or frozen for cytokine array analysis. The corneal sections were IHC stained for COX-2, MMP-9, and VEGF expression as detailed under the "Materials and Methods" section. Representative images showing an increase in COX-2 expression (A) following NM exposure. IL-8 levels in corneal lysates at 3-day post-NM exposure (B). Representative pics for MMP-9 staining (C) and MMP-9 levels in corneal lysates at 3-day post NM-exposure (D). Representative images showing VEGF expression (E) and bar diagram showing quantification of the staining (F; no control bars at day 14 indicate that there was no significant VEGF staining observed in control corneas) following NM exposure. Representative control images are from 3-day post NM exposure. Data presented are mean ± SEM (n = 3). *, $p < 0.05$ compared to the control group. e, epithelium; s, stroma; size bar, 50 μm.

was also increased at days 14 and 28 post NM-exposure [staining grade was ~0.5 and ~1 at day 14 and 28 post NM-exposure respectively, compared to negligible staining (grade 0) in control group] with significant increased observed at day-14 post NM-exposure (Fig. 4E & F).

4. Discussion

Vesicating agent SM continues to be a potential threat in conflicts, warfare, and terrorism, due to the devastating injuries it causes, relatively easy synthesis and lack of antidotes (Geraci, 2008; Ghabili et al., 2011; Graham and Schoneboom, 2013). In spite of extensive research efforts to understand the injury mechanisms and develop an effective therapy, the pathways leading to injury are still unclear and there are no approved antidotes to effectively treat the inflicted injuries (Graham and Schoneboom, 2013; Kadar et al., 2009; Kehe et al., 2009; Kehe and Szinicz, 2005; Shakarjian et al., 2010). Based on the reports from battlefield injuries, ocular tissue is highly sensitive to SM exposure with injury occurring at much lower concentration compared to other organs (Papirmeister et al., 1991).

To study vesicating agents-induced ocular injury, we have used NM as a surrogate for SM. NM, like SM, is a highly reactive, bifunctional alkylating vesicating agent and covalently modifies all major molecules in the cell causing injuries comparable to SM (Banin et al., 2003; Morad et al., 2005; Olajos et al., 1998). Although both NM and SM are primarily alkylating agents, however, due to differences in their chemical nature, they could have different cellular targets resulting in variable injury outcomes. NM has been shown to modify Lys, His, and Cys residues *via* aziridinium formation, followed immediately by covalent reaction (Thompson and DeCaprio, 2013). Thus, once inside the cell, NM may cause irreversible cellular damage by modification of Cys containing proteins. Since use of SM in laboratory settings is highly restricted, NM has been used by us and several other groups to decipher under lying mechanism of mustard vesicants-induced ocular injuries (Banin et al., 2003; Gordon et al., 2016; Gordon et al., 2010; Goswami et al., 2018; Goswami et al., 2016b; Morad et al., 2005; Tewari-Singh et al., 2012). The injury observed in our studies and the endpoints of study relate to the ocular SM exposure in humans including the clinical outcomes (Kadar et al., 2009; Panahi et al., 2017; Panahi et al., 2018).

In our earlier studies we have evaluated NM-induced injury in HCE cells and *ex vivo* rabbit cornea organ culture (Goswami et al., 2018; Goswami et al., 2016b; Tewari-Singh et al., 2012). To more directly relate our work to future care of patients, we have moved our studies to an acute corneal injury *in vivo* rabbit model. The results from NM exposure in NZW rabbits here provide clinical, biological, and molecular changes associated with NM-induced acute corneal injury. NM exposure led to eyelid swelling, ocular edema and inflammation, conjunctivitis, hunched posture, thick whitish/yellow ocular discharge, matted fur around the eye, and severe corneal injury. The injury parameters, comprising of increase in corneal thickness, corneal opacity, epithelial degradation, death of keratocytes, influx of inflammatory cells, epithelial-stromal separation, increase in COX-2, VEGF, MMP-9, and IL-8 levels, corroborate earlier ocular injury studies carried out with SM and NM (Banin et al., 2003; Morad et al., 2005; Tewari-Singh et al., 2017). Involvement of similar pathways has been observed in our studies with SM (unpublished data) and LEW-induced ocular injury (Tewari-Singh et al., 2016; Tewari-Singh et al., 2017) although the severity and timing of the injury parameters are different.

Significant corneal ulceration and corneal opacity starting from day 3 post NM-exposure could be due to the death/removal of the epithelial layer, thereby altering the permeability and barrier function of the cornea. The degradation of the epithelium could be attributed to the alkylating properties of NM as well as oxidative stress-mediated membrane damage (Thavaselvam and Flora, 2014). As observed earlier in HCE cells and *ex vivo* studies in rabbit cornea, NM exposure reduced HCE cell viability and caused significant apoptotic cell death in *ex vivo* rabbit cornea. In addition to the epithelial cell degradation and cell death, the epithelial layer histology further suggests that NM decreased the epithelial cell proliferation and differentiation. Once the epithelial barrier is perturbed, the hydration state of the cornea could be compromised resulting in increased corneal stromal thickness as was observed in the present as well as in previous studies (Costagliola et al., 2013). The influx of inflammatory cells could further lead to the increase in corneal thickness. Similar increase was observed in our earlier reported studies with LEW (Tewari-Singh et al., 2017). As reported previously in our studies with LEW, a significant decrease in keratocyte number was observed upon NM exposure (Tewari-Singh et al., 2017). The population of stromal keratocytes is known to decrease in severe chemical injuries, initiating the degradation of collagen fibrils (West-Mays and Dwivedi, 2006). This compromises the structural integrity of the corneal stroma and could result in corneal ulceration and perforation (West-Mays and Dwivedi, 2006). Keratocytes are responsible for collagen synthesis and are critical for maintenance and regeneration of the stroma (West-Mays and Dwivedi, 2006). However, ascorbate is required for collagen synthesis. A decrease in ascorbic acid levels in the anterior chamber of the eye upon SM exposure has been observed which could be ROS mediated (Banin et al., 2003; Panahi et al., 2013).

An inflammatory response is the major event following mustard vesicating agents' exposure in the cornea (Horwitz et al., 2019; Horwitz et al., 2018). COX-2, an inducible enzyme involved in prostaglandin biosynthesis that has been shown to play a role in vesicant induced cutaneous injury (Kehe and Szinicz, 2005; Shakarjian et al., 2010), was found to be upregulated following NM ocular exposure. Our results here further support our previous reported increase in COX-2 expression in HCE cells and in *ex vivo* rabbit cornea (Goswami et al., 2018; Goswami et al., 2016b; Tewari-Singh et al., 2012). An increase in prostaglandin synthesis results in an influx of inflammatory cells and thus suggests a role of COX-2 in NM induced inflammation. In addition, inflammation can play an important role in angiogenesis following NM exposure in the cornea because COX-2 is reported to cause VEGF expression by inducing the expression of VEGF genes (Gonzalez et al., 2013). Increase in IL-8, a chemokine that attracts leukocytes to the injury site and acts as a mediator of angiogenesis (Koch et al., 1992), was also found to be upregulated upon NM exposure in the rabbit cornea. IL-8 has been shown to be upregulated in SM- and LEW-induced ocular injury (Ghasemi et al., 2013; Tewari-Singh et al., 2017). The significant increase in inflammatory cells in the stroma could be due to increased expression of COX-2 and elevated IL-8 levels in the cornea.

The role of MMPs has been well established in SM- and NM-induced ocular and skin injuries, causing degradation of extracellular matrix, vesication, and cell death. MMPs, specifically MMP-9, has been found to be elevated upon SM/NM exposure in animal models as well as in the serum of warfighters exposed to SM (Gordon et al., 2010; Kehe et al., 2009; Shakarjian et al., 2006; Shakarjian et al., 2010; Shohrati et al., 2014). Hence in the current study, the elevated levels of MMP-9 in the cornea upon NM exposure further confirms MMP-9 as a key mediator in NM induced inflammation and epithelial-stromal separation. In addition, recent study in the eye reports that vesicating agents can lead to the cleavage of transmembrane hemidesmosomal collagen XVII, a component anchoring the epithelium to the stroma, which could partially cause epithelial-stromal separation (DeSantis-Rodrigues et al., 2016). Neovascularization is one of the delayed effect of SM exposure in animal models as well as in humans (Amir et al., 2000; Ghasemi et al., 2013; Kadar et al., 2014; Kadar et al., 2001). In our previous studies in HCE cells and *ex vivo* rabbit cornea culture we did see an increase in VEGF (an angiogenic mediator) expression (Goswami et al., 2018; Goswami et al., 2016b; Tewari-Singh et al., 2012). Apart from promoting angiogenesis, VEGF plays an important role in repair mechanisms (Eming and Krieg, 2006). In the present study, we didn't see significant corneal neovascularization upon NM exposure. However, some increase in VEGF expression was observed at day 28 post-exposure that could be related to the increase in blood vessels observed at day 28 post NM-exposure in the stroma.

In summary, the development of this *in vivo* model for NM-induced acute corneal injury and the relevant clinical, biological, and molecular markers of the injury could be helpful in screening of potential therapies.

Funding information

This work was supported by the Countermeasures Against Chemical Threats (CounterACT) Program, Office of the Director National Institutes of Health (NIH) and the National Eye Institute (Grant Number U01EY023143) and by a Challenge Grant to the Department of Ophthalmology from Research to Prevent Blindness.

Declaration of interest

None.

References

Amir, A., et al., 2000. Beneficial effects of topical anti-inflammatory drugs against sulfur mustard-induced ocular lesions in rabbits. J. Appl. Toxicol. 20 (Suppl. 1), S109–S114.
Anumolu, S.S., et al., 2010. Doxycycline loaded poly(ethylene glycol) hydrogels for healing vesicant-induced ocular wounds. Biomaterials. 31, 964–974.
Balali-Mood, M., Hefazi, M., 2006. Comparison of early and late toxic effects of sulfur mustard in Iranian veterans. Basic Clin. Pharmacol. Toxicol. 99, 273–282.
Balali-Mood, M., et al., 2011. Delayed toxic effects of sulfur mustard on respiratory tract of Iranian veterans. Hum. Exp. Toxicol. 30, 1141–1149.
Banin, E., et al., 2003. Injury induced by chemical warfare agents: characterization and treatment of ocular tissues exposed to nitrogen mustard. Invest. Ophthalmol. Vis. Sci. 44, 2966–2972.
Costagliola, C., et al., 2013. Corneal oedema and its medical treatment. Clin. Exp. Optom. 96, 529–535.
DeSantis-Rodrigues, A., et al., 2016. ADAM17 inhibitors attenuate corneal epithelial detachment induced by mustard exposure. Invest. Ophthalmol. Vis. Sci. 57, 1687–1698.
Eming, S.A., Krieg, T., 2006. Molecular mechanisms of VEGF-A action during tissue repair. J. Investig. Dermatol. Symp. Proc. 11, 79–86.
Geraci, M.J., 2008. Mustard gas: imminent danger or eminent threat? Ann. Pharmacother. 42, 237–246.
Ghabili, K., et al., 2010. Mustard gas toxicity: the acute and chronic pathological effects. J. Appl. Toxicol. 30, 627–643.
Ghabili, K., et al., 2011. Sulfur mustard toxicity: history, chemistry, pharmacokinetics, and pharmacodynamics. Crit. Rev. Toxicol. 41, 384–403.

Ghasemi, H., et al., 2009. Systemic and ocular complications of sulfur mustard: a panoramic review. Toxin Rev. 28, 14–23.
Ghasemi, H., et al., 2013. A clinicopathological approach to sulfur mustard-induced organ complications: a major review. Cutan. Ocul. Toxicol. 32, 304–324.
Gonzalez, L., et al., 2013. Nanotechnology in corneal neovascularization therapy—a review. J. Ocul. Pharmacol. Ther. 29, 124–134.
Gordon, M.K., Enzenauer, R.W., Babin, M.C., 2009. Ocular toxicity of sulfur mustard. In: Gupta, R.C. (Ed.), Handbook of Toxicology of Chemical Warfare Agents. Elsevier Inc, pp. 575–594.
Gordon, M.K., et al., 2010. Doxycycline hydrogels as a potential therapy for ocular vesicant injury. J. Ocul. Pharmacol. Ther. 26, 407–419.
Gordon, M.K., et al., 2016. The molecules in the corneal basement membrane zone affected by mustard exposure suggest potential therapies. Ann. N. Y. Acad. Sci. 1378, 158–165.
Goswami, D.G., et al., 2016a. Corneal toxicity induced by vesicating agents and effective treatment options. Ann. N. Y. Acad. Sci. 1374, 193–201.
Goswami, D.G., et al., 2016b. Nitrogen mustard-induced corneal injury involves DNA damage and pathways related to inflammation, epithelial-stromal separation, and neovascularization. Cornea. 35, 257–266.
Goswami, D.G., et al., 2018. Efficacy of anti-inflammatory, antibiotic and pleiotropic agents in reversing nitrogen mustard-induced injury in ex vivo cultured rabbit cornea. Toxicol. Lett. 293, 127–132.
Graham, J.S., Schoneboom, B.A., 2013. Historical perspective on effects and treatment of sulfur mustard injuries. Chem. Biol. Interact. 206, 512–522.
Horwitz, V., et al., 2014. The beneficial effects of doxycycline, an inhibitor of matrix metalloproteinases, on sulfur mustard-induced ocular pathologies depend on the injury stage. Curr. Eye Res. 39, 803–812.
Horwitz, V., et al., 2018. Differential expression of corneal and limbal cytokines and chemokines throughout the clinical course of sulfur mustard induced ocular injury in the rabbit model. Exp. Eye Res. 177, 145–152.
Horwitz, V., et al., 2019. A comprehensive analysis of corneal mRNA levels during sulfur mustard induced ocular late pathology in the rabbit model using RNA sequencing. Exp. Eye Res. 184, 201–212.
Kadar, T., et al., 2001. Characterization of acute and delayed ocular lesions induced by sulfur mustard in rabbits. Curr. Eye Res. 22, 42–53.
Kadar, T., et al., 2009. Ocular injuries following sulfur mustard exposure—pathological mechanism and potential therapy. Toxicology. 263, 59–69.
Kadar, T., et al., 2011. Delayed loss of corneal epithelial stem cells in a chemical injury model associated with limbal stem cell deficiency in rabbits. Curr. Eye Res. 36, 1098–1107.
Kadar, T., et al., 2013. Prolonged impairment of corneal innervation after exposure to sulfur mustard and its relation to the development of delayed limbal stem cell deficiency. Cornea. 32, e44–e50.
Kadar, T., et al., 2014. Anti-VEGF therapy (bevacizumab) for sulfur mustard-induced corneal neovascularization associated with delayed limbal stem cell deficiency in rabbits. Curr. Eye Res. 39, 439–450.
Kehe, K., Szinicz, L., 2005. Medical aspects of sulphur mustard poisoning. Toxicology. 214, 198–209.
Kehe, K., et al., 2009. Molecular toxicology of sulfur mustard-induced cutaneous inflammation and blistering. Toxicology. 263, 12–19.
Koch, A.E., et al., 1992. Interleukin-8 as a macrophage-derived mediator of angiogenesis. Science. 258, 1798–1801.
Mansour Razavi, S., et al., 2012. A review on delayed toxic effects of sulfur mustard in Iranian veterans. Daru. 20, 51.
McNutt, P., et al., 2012. Pathogenesis of acute and delayed corneal lesions after ocular exposure to sulfur mustard vapor. Cornea. 31, 280–290.
Morad, Y., et al., 2005. Treatment of ocular tissues exposed to nitrogen mustard: beneficial effect of zinc desferrioxamine combined with steroids. Invest. Ophthalmol. Vis. Sci. 46, 1640–1646.
Olajos, E., et al., 1998. Acute inhalation toxicity of neutralized chemical agent identification sets (CAIS) containing agent in chloroform. J. Appl. Toxicol. 18, 363–371 Wiley Online Library.
Panahi, Y., et al., 2013. Review article: ocular effects of sulfur mustard. Iran. J. Ophthalmol. 25, 90–106.
Panahi, Y., et al., 2017. Sulfur mustard-induced ocular injuries: update on mechanisms and management. Curr. Pharm. Des. 23, 1589–1597.
Panahi, Y., et al., 2018. Sulfur mustard-related ocular complications: a review of proteomic alterations and pathways involved. Curr. Pharm. Des. 24, 2849–2854.
Papirmeister, B., Feister, A.J., Robinson, S.I., Ford, R.D., 1991. Medical Defense against Mustard Gas, Toxic Mechanisms and Pharmacological Implications. CRC press.
Saladi, R.N., et al., 2006. Mustard: a potential agent of chemical warfare and terrorism. Clin. Exp. Dermatol. 31, 1–5.
Shakarjian, M.P., et al., 2006. Preferential expression of matrix metalloproteinase-9 in mouse skin after sulfur mustard exposure. J. Appl. Toxicol. 26, 239–246.
Shakarjian, M.P., et al., 2010. Mechanisms mediating the vesicant actions of sulfur mustard after cutaneous exposure. Toxicol. Sci. 114, 5–19.
Shohrati, M., et al., 2014. Serum matrix metalloproteinase levels in patients exposed to sulfur mustard. Iran Red Crescent Med J 16, e15129.
Smith, K.J., Skelton, H., 2003. Chemical warfare agents: their past and continuing threat and evolving therapies. Part I of II. Skinmed. 2, 215–221.
Tewari-Singh, N., et al., 2012. Silibinin, dexamethasone, and doxycycline as potential therapeutic agents for treating vesicant-inflicted ocular injuries. Toxicol. Appl. Pharmacol. 264, 23–31.
Tewari-Singh, N., et al., 2016. Clinical progression of ocular injury following arsenical vesicant lewisite exposure. Cutan. Ocul. Toxicol. 1–10.
Tewari-Singh, N., et al., 2017. Histopathological and molecular changes in the rabbit cornea from arsenical vesicant lewisite exposure. Toxicol. Sci. 160, 420–428.
Thavaselvam, D., Flora, S.S., 2014. Chapter 30—Chemical and biological warfare agents. In: Gupta, R.C. (Ed.), Biomarkers in Toxicology. Academic Press, Boston, pp. 521–538.
Thompson, V.R., DeCaprio, A.P., 2013. Covalent adduction of nitrogen mustards to model protein nucleophiles. Chem. Res. Toxicol. 26, 1263–1271.
Wattana, M., Bey, T., 2009. Mustard gas or sulfur mustard: an old chemical agent as a new terrorist threat. Prehosp. Disaster Med. 24, 19–29 (discussion 30-1).
West-Mays, J.A., Dwivedi, D.J., 2006. The keratocyte: corneal stromal cell with variable repair phenotypes. Int. J. Biochem. Cell Biol. 38, 1625–1631.
WHO, 2004. WHO Guidance: Public Health Response to Biological and Chemical Weapons. WHO, Geneva Switzerland.